RSC Advances

PAPER

View Article Online
View Journal | View Issue

Cite this: *RSC Adv.*, 2014, **4**, 11438

Toxicity of high glycolic poly(DL-lactic-*co*-glycolic acid) stabilized ruthenium nanoparticles against human promyelocytic leukemia cells†

Venkatesan Nandakumar,[a] Venkatesan Vettriselvi[b] and Mukesh Doble*[a]

Received 29th November 2013
Accepted 13th January 2014

DOI: 10.1039/c3ra47142j

www.rsc.org/advances

High glycolic poly-(lactic-*co*-glycolic acid) stabilized ruthenium nanoparticles were toxic towards human promyelocytic leukemia cells (HL60) and the mode of cell death was by apoptosis and in contrast it was not toxic towards blood lymphocytes. There was a significant increase in the oxidative stress within these cells and the toxicity of nanoparticles towards HL 60 cells could be attributed to the TGF β mediated signal transduction. This study indicated that such polymer stabilized ruthenium nanoparticles could be used as a selective anticancer agent.

The unique physico-chemical properties of metal nanoparticles have drawn considerable attention in both industrial and biomedical fields.[1,2] Some metals that are extensively studied as nanoparticles include silver, gold, platinum, titanium and rhodium.[3–6] But the use of nanoparticles is restricted due to their tendency to undergo aggregation. This issue is addressed by developing polymer stabilized metal nanoparticles. The polymer acts as a stabilizing medium and prevents aggregation and uncontrollable growth. PVC is used as a stabilizing medium for platinum and copper nanoparticles, it decreases the aggregation of the metals and increases their surface area. Palladium nanoparticles are stabilized with Nafion (a sulfonated tetrafluoroethylene polymer). The polymer support helps to measure the concentration of glucose in the vicinity of the metal, without interference from oxygen, ascorbic acid and uric acid. Gold and silver nanoparticles have been stabilized by polyvinyl alcohol (PVA), polyvinyl pyrolidone (PVP), pullulan, chitosan, and polylactic acid (homopolymer and co-polymer).[7–9] PLGA with a high lactic/glycolic acid (L/G) ratio and PLA are used as stabilizing agents to achieve longer circulation times.[8] Submicron PLA and PLGA are widely tested as non-viral vectors for the delivery of biomolecules.[7]

Ruthenium was selected in the current study because in contrast to other existing conventional nanoparticles there has not been much attention paid to its biomedical applications.[2] Ruthenium nano-catalysts synthesized by conventional chemical vapor deposition have been used in fuel cells, capacitors[10,11] and so on. Other preparation methods have limitations for the synthesis of highly dispersed nanoparticles.[12] Ruthenium based metal complexes have been extensively studied for anticancer therapeutics.[13] With nitrogen ligands, they localize within the cancer cells and exhibit cytotoxicity and they have been found to be better alternatives than the existing anticancer drugs.[13]

The enantioselective recognition of DNA by polypyridyl ruthenium complexes is used as a probe for analyzing the conformation of the former.[14–16] The pharmacological profile of two ruthenium(III) compounds, imidazolium *trans*-[tetrachloro(DMSO)(imidazole)ruthenate(III)] (NAMI-A) and indazolium *trans*-[tetrachlorobis(1*H*-indazole)ruthenate(III)] (KP-1019), are extensively studied.[17] The cytotoxic activities of these complexes are attributed to their ability to form adducts with DNA and protein kinases and by apoptosis.[18] These complexes are known to induce mitochondrial mediated and caspase dependent apoptosis[18] and induce autophagy[19] in tumor cells. Cytokines are molecular messengers that allow the cells of the immune system to communicate with one another to generate a response to the target antigen. Although many forms of communication within the immune system occur through direct cell–cell interactions, cytokines enable the rapid propagation of an immune signal. So there is a growing interest in harnessing the immune system to eradicate cancer.

In view of its high propensity to react and bind to DNA and its cytotoxic profile, the present study is aimed at understanding the effect of ruthenium nanoparticles stabilized by poly-(DL-lactic-*co*-glycolic acid) (10:90) on human blood lymphocytes and human promyelocytic leukemia cells. High glycolic PLGA is used as a carrier for nanoparticle pertaining to its faster degradation rate, so that the bioavailability of metal nanoparticles is reduced

[a]*Department of Biotechnology, Indian Institute of Technology Madras, Chennai, Tamilnadu, India. E-mail: mukeshd@iitm.ac.in; Tel: +914422574107*

[b]*Department of Human Genetics, Sri Ramachandra University, Chennai, India*

† Electronic supplementary information (ESI) available: Includes physico-chemical characteristics of the nanoparticles including IR spectrum (S1), particle size distribution (S2), thermogravimetric analysis of polymer (S3) and polymer metal nanoparticle (S4), cytotoxicity of the nanoparticle (S5) and intracellular ROS generation in HL 60 cells (S6), cytotoxicity of the nanoparticle (S7) and intracellular ROS generation in peripheral blood lymphocytes (S8). See DOI: 10.1039/c3ra47142j

which would alleviate the problem of systemic cytotoxicity of these metal nanoparticles to the other cells. The biocompatible and biodegradable property of the polymer makes it more suitable for drug delivery than other carriers for many biomedical applications.[20,21] In addition this polymer can be used to passivate metal nanoparticles.[22]

Result & discussion

Characterization

With the increase in time, the absorbance peak at 410 nm for ruthenium chloride decreases gradually upon adding $NaBH_4$, with no obvious absorption peak it confirms complete reduction of trivalent ruthenium to zerovalent (Fig. 1). The IR spectrum (ESI Fig. S1†) for Ru–PLGA 10:90 has peaks corresponding to OH (3406 cm^{-1}), CH (2957 cm^{-1}), CO (1744 cm^{-1}), and COC (1092 cm^{-1}), which are characteristic of the polymer, also a stretch at 2042 cm^{-1} confirms the presence of ruthenium. The TEM micrographs (Fig. 2) confirm the size of the zerovalent ruthenium and the average size of the immobilized ruthenium is determined from particle size analyzer (ESI Fig. S2†). The TGA thermogram of the PLGA 10:90 and PLGA 10:90 Ru nanoparticles (ESI Fig. S3 and S4†) shows the thermal stability. Complete decomposition of the PLGA 10:90 polymer and the polymer–metal nanoparticle was observed at 340 and 365 °C. The increase in the thermal stability of the latter when compared to the former could be attributed to the presence of the metal.

Cytotoxicity

The nanoparticles were cytotoxic to HL 60 cells at all the tested concentrations and the percentage cell viability varies in a concentration dependent manner and there is significant difference between the concentrations tested ($p = 0.001$) (ESI Fig. S5†). Maximum cell death was observed at a concentration of 500 μg ml^{-1}, which was chosen for further studies. In the case of lymphocytes, the cells were viable even after 24 hours and there was no statistically significant effect on the cell viability at any of the concentrations tested ($p = 0.357$) (ESI Fig. S7†).

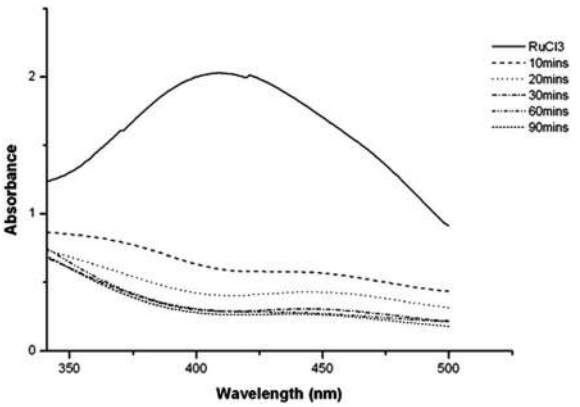

Fig. 1 UV-visible spectra of *in situ* reduction of Ru^{3+} to Ru^0 stabilized by PLGA 10:90.

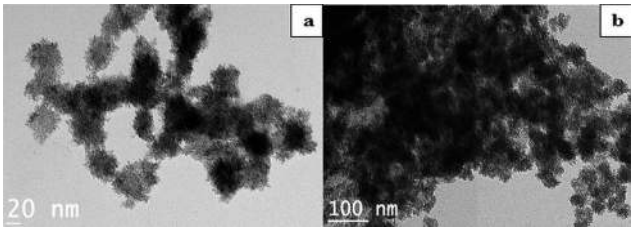

Fig. 2 TEM micrographs of ruthenium immobilized on PLGA 10:90 (a and b).

Fig. 3a & b show the live peripheral blood lymphocyte cells treated with PLGA 10:90 Ru nanoparticles and the Fig. 3c & d show the mixture of live and dead HL 60 cells after treatment. Acridine orange emits green fluorescence upon binding to the DNA whereas ethidium bromide gives red fluorescence when bound to the nuclei of dead cells. From these figures it is clear that the ruthenium nanoparticles are non-toxic to the lymphocytes but it is toxic to the leukemic cells. The condensed nuclei and lysed cell membrane in the case of ruthenium treated HL 60 cells stained red indicate late apoptosis (Fig. 3d). The mode of induction and mechanism underlying nanoparticle mediated cytotoxicity was analyzed by the intra cellular ROS levels and inflammatory cytokine expression.

Levels of intracellular ROS

The nanoparticles induce oxidative stress in a dose dependent manner and there was significant difference between the concentrations tested ($p = 0.013$), with the increase in concentration there was an increase in the peroxide levels. At the highest concentration (500 μg ml^{-1}) tested the intracellular peroxide levels increased three fold when compared to that of untreated HL 60 cells (ESI Fig. S6†). Oxidative stress is also induced in lymphocytes and it is marginally less when compared to that induced in HL 60 cells (ESI Fig. S8†). There exists a very close relation between ROS, mitochondrial transmembrane potential and apoptosis,[23] and their levels play an important role in mitochondrial damage mediated cell death.[24] The electron transport chain in mitochondria is the major source for ROS generation and increased oxidative stress acts as

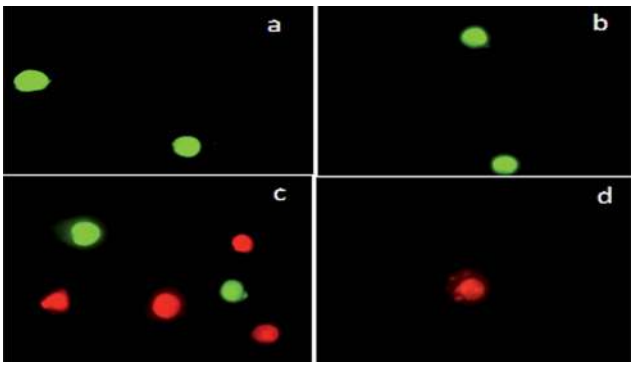

Fig. 3 Effect of Ru-PLGA 10:90 treated peripheral blood lymphocytes (a and b) and HL 60 cells (c and d).

an endogenous source for mitochondrial DNA damage.[25] Literature states that accumulation of ROS activates the members of the stress related protein kinase (including c JUN NH_2-terminal kinase) resulting in cell death.[23]

Analysis of cytokine expression

Cytokines are endogenous inflammatory and immune-modulating mediators primarily involved in the growth processes and in host responses to tissue injury, infections and many diseases. Cytokines are known to exhibit both negative and positive regulatory effects on various target cells. The present study analyses the inducers of cell death, particularly the secretary cytokines and the transcription factors that regulate the expression of these cytokines. The effect of nanoparticles on these cells depends on their synthesis method, size and the extent of aggregation.[26] The expression of proinflammatory cytokines in HL 60 cells and human blood lymphocytes after treatment with nanoparticles are shown in Fig. 4 & 5. The expressions are plotted using the $2^{-\Delta\Delta CT}$ values of polymer treated (control) and ruthenium immobilized polymer carrier, whose ΔCT values are obtained after subtracting the CT of endogenous control (β actin) from the target gene's CT values.

In the current study there is a significant increase in the expression of anti-inflammatory cytokines including TGF β1, β2 and β3. TGF β1 is multifunctional in nature, which is responsible for the balance between many cellular responses including growth arrest, differentiation and induction of apoptosis in both normal and cancer cells.[27,28] It has been proved that TGF β1 induces cell death in L1210 cells (leukemic cells) by triggering apoptosis or cell cycle arrest at the G1–S phase, where the primary response is triggered by the pro-apoptotic bax gene and it is also marked by the decreased expression of anti-apoptotic bcl2 genes.[28] The decreased expression of proinflammatory cytokines together with the cytotoxic profile in the present study could be attributed to the apoptotic role of TGF β1. TGF β1 mediated apoptosis *via* Smad7 gene (mothers against decapentaplegic homolog 7) has been reported in many cancer cells including prostate cancer cell lines.[29] TGF β2 also plays an important role in inducing apoptosis in a murine model.[30] TGF β3 is also known to induce Fas independent apoptosis in chronic myelogenous leukemia cells.[31]

The expressions of transcription factor NFκB in peripheral blood lymphocytes are significantly higher than cytokines, which is followed by IFN, TNF-α and FasL. Activation of the transcription factor NFκB has been attributed to the dual roles of both pro-apoptosis and anti-apoptosis. The exact role of this transcription factor depends on cell type and the nature of stimuli that induce apoptosis.[32] Increased expression of IL1 and TNF-α are known to activate and induce the expression of NFκB, which in turn act as a proinflammatory cytokine transcription factor resulting in further up regulation of IL1 and TNF-α. This also protects the cells from apoptosis. This could be the reason for the absence of cell death observed in the peripheral blood lymphocytes (Fig. 3a & b). This further explains the anti-apoptotic role of the biphasic NFκB.[33] It is also reported that the anti-apoptotic role of NFκB is effective only if it acts through IκBα tyrosine kinase pathways which explains that the pathway of activation is an important parameter that determines the role of NFκB.[33]

Interferon γ (IFN γ) is also significantly expressed in the case of peripheral blood lymphocytes. The interaction between IFN and different types of receptor triggers different response in cells.[34] The differential (higher) expression of the interferon receptor, IFN γR_2 on the cell surface determines whether the cells should undergo apoptosis or proliferation. The high expression of IFN observed in our case together with the viable cells (non-apoptotic) we propose that IFN γ does not induce apoptosis (should be further confirmed based on the mRNA expression of IFN γR_2).

Metal nanoparticles mediated targeted cytotoxicity of cancer cells is widely researched in order to reduce the toxicity of organo-metallic complexes towards normal cells. Apoptosis can either be through an extrinsic or intrinsic pathway, but nanoparticle mediated cytotoxicity triggers both the pathways. On the contrary the oxidative stress induced intracellular DNA damage leading to apoptosis favors the intrinsic pathway, which is reported and proved for most metal nanoparticles.[35] Ruthenium, belongs to the platinum group of metals, which are known to trigger cell death by the apoptotic pathway during photothermal treatment.[36,37] Ruthenium-106 is also used in the brachytherapy for retinoblastoma, since it emits β rays with fewer secondary consequences.[38] The β rays with a high energy ionize the cells and form free radicals resulting in oxidative

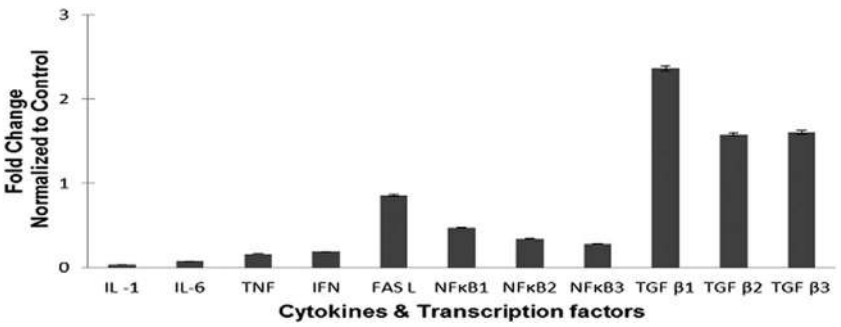

Fig. 4 Normalized fold expression of cytokines and transcription factors in HL 60 after exposure to nanoparticles ($p < 0.05$) (results are normalized to control).

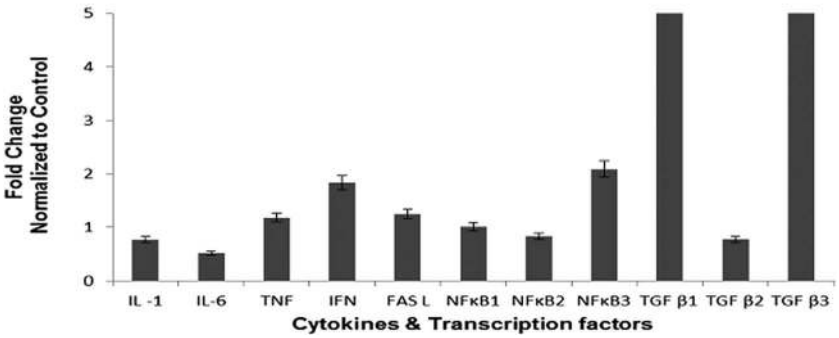

Fig. 5 Normalized fold expression of cytokines and transcription factors in peripheral blood lymphocytes after exposure to nanoparticles ($p < 0.05$) (results are normalized to control).

stress induced apoptosis of ruthenium nanoparticles leading to programmed cell death (apoptosis).

Materials & methods

Materials

Ruthenium(III) chloride (Avra synthesis, India), poly-lactic acid, and poly-(DL-lactic-*co*-glycolic acid) 10:90. Tetrahydrofuran (Fischer Scientific, India), trifluoroaceticacid (Fischer Scientific, India), oligonucleotide primers (Genei, Bangalore, India), TRIzol® (Invitrogen, USA).

Cells and culture medium: HL 60 (Human promyelocytic leukemia cells) (NCCS, Pune India) and normal human blood lymphocytes (healthy volunteer). Roswell park memorial institute medium (RPMI) and antibiotic antimycotic solution (HiMedia, India), fetal bovine serum (Gibco®, India).

Preparation of ruthenium immobilized polymer particles

Synthesis of PLGA was reported in our previous study.[39] Ruthenium immobilized polymer nanoparticles were prepared based on an earlier reported method.[40] 100 mg of polymer was solubilized in a mixture of tetrahydrofuran and trifluoroacetic acid in the ratio of 9 : 1 in a 250 ml round bottom flask and purged with nitrogen for 1 h with continuous stirring. Ruthenium(III) chloride (5 mg, 1.5×10^{-4} mol) dissolved in deionized water was added and stirred continuously for 1 h. Then 2 molar equivalents of sodium borohydride was added and stirred for 6 h at room temperature. The reduction of ruthenium chloride to zerovalent ruthenium was monitored periodically with a UV-visible spectrophotometer (Jasco V 550). The resulting dark brown spheres were separated by centrifugation (12 000 rpm, 30 min) and repeatedly washed with ethanol.

Characterization

The particles were characterized by FT-IR spectroscopy (Perkin Elmer Spectrum) operated in transmittance mode in the range of 400–4000 cm^{-1} with a resolution of 4 cm^{-1}. The surface morphology of the particles was analyzed under transmission electron microscope (TEM CM20). The mean size of ruthenium immobilized polymeric particles was estimated with the help of Zetatrac particle size Analyzer (Microtrac Inc. USA). Thermogravimetric analysis of the nanoparticles was carried out under nitrogen atmosphere from 25 to 500 °C at a constant heating rate of 10 °C min^{-1} (TGA Q500 V20.10 Universal TA instrument).

Cytotoxicity of PLGA stabilized ruthenium nanoparticles

The human promyelocytic leukemia cells (HL 60) were cultured on T75 polystyrene flasks in RPMI 1640 medium supplemented with 1% antibiotic and antimycotic solution and 10% fetal bovine serum (FBS) until it reached confluence. Later the cells were counted with the help of hemocytometer and approximately 10^4 cells were seeded into a 96 well tissue culture plate. 24 h after incubation, the cells were treated with different concentrations (500, 400, 300, 200, 100, 10 μg ml^{-1}) of ruthenium immobilized nanoparticles. The cell viability was determined based on a standard procedure, which measured the reduction of MTT, a tetrazolium salt to insoluble precipitate.[41] The results are expressed as percentage of viable cells with respect to the control (untreated cells).

Similarly peripheral blood lymphocytes were isolated from blood samples collected from healthy human volunteers by using HiSep™ LSM (HiMedia) according to the manufacturer's protocol. Approximately 10^4 cells were seeded into a 96 well plate and treated with a similar concentration of ruthenium immobilized nanoparticles and the percentage cell viability was determined by MTT assay. The results are expressed after normalizing to control.

Approximately 5000 cells were seeded in a 6-well plate and when 80% confluent they were treated with the nanoparticle (500 μg ml^{-1}). After 24 hours of incubation the cells were washed with DPBS thrice and stained with ethidium bromide (EtBr) and acridine orange (AcO). The morphology of the cells was visualized under a fluorescent microscope (Leica 4200, Germany).

Determination of intracellular ROS

The amount of intracellular ROS generated in both the lymphocytes and HL 60 cells was determined with the help of cell permeable non-fluorescent 2,7-dichlorohydrofluorescein di acetate (DCF 2 DA) dye. ROS converts this dye to a highly fluorescent 2,7-dichlorofluorescein by ROS.[42] In brief cells were

treated with different concentrations of nanoparticles (500, 400, 300, 200, 100, 10 μg ml^{-1}) for 24 hours and then incubated with 10 μM of DCF 2 DA for 15 min, washed with PBS and the amount of fluorescence generated is measured with the help of an Enspire Multimode plate reader (Perkin Elmer, Singapore). The results are expressed as fold increase normalized to control.

Exposure to nanoparticles and RNA isolation

Peripheral blood samples isolated from healthy human volunteers were suspended in RPMI 1640 medium supplemented with 1% antibiotic and antimycotic solution, 2 mM glutamine, and 10% fetal bovine serum (FBS). Cells were divided into three groups, of which two groups were treated with 500 μg of the polymer stabilized metal nanoparticles and polymer alone. One group left untreated was used as the control. They were incubated for 24 h and the total RNA from all the samples was isolated. Similar experiments were carried out with HL 60 cells.

Materials used for RNA extraction were pre-treated with diethylpyrocarbonate (DEPC) and RNA isolation was carried out using TRIzol® reagent (according to manufacturer's protocol). The isolated mono-nuclear cells were mixed with 500 μl of TRIzol reagent, vortexed for 30 s and incubated for 5 min at room temperature. Later 1 ml of chloroform was added and vortexed for 30 s. Then it was incubated for 5 minutes at room temperature and centrifuged at 10 000 rpm for 10 minutes at 4 °C. RNA from the clear supernatant was precipitated using isopropyl alcohol, and further centrifuged at 12 000 rpm for 15 minutes at 4 °C. The precipitated RNA was resuspended in 70% ethanol. RNA quantity and integrity was determined using a NanoDrop analyzer at 260 and 280 nm and also by agarose gel electrophoresis. The RNA was resuspended in 100 μl of nuclease free water and stored at −80 °C until further use. The total RNA (1 μg) isolated was reverse-transcribed to cDNA using a high cDNA reverse transcriptase kit (Applied Biosystems).[43] The reaction mixture was incubated for 10 min at 25 °C and the reaction was terminated by heating at 85 °C for 5 min. The cDNA was stored at −80 °C until further use.

Real-time PCR analysis

Real time-PCR amplification was performed on 9700 HT RT-PCR, Applied Biosystem, UK.[43] Reactions were carried out in a total volume of 20 μl, containing 2 μl cDNA template, 10 μl SYBR Green Supermix, 0.5 μl each of the primer (10 μM) and 2 μl of sterile water. All the reactions were run in triplicate and the conditions used included an initial denaturation at 95 °C for 2 min followed by 95 °C for 11 min and an extension at 60 °C for 1 min. The amplification was repeated 40 times. The process was also performed on reaction mixture cDNA as negative controls. The expression of the target gene was normalized to the endogenous control β-actin and was represented relative to the control and was determined by the $2^{-\Delta\Delta CT}$ method.

Statistical analysis

All the statistical analyses were carried out with the help of SYSTAT version 13 (Systat software Inc., USA) with a 95% confidence level.

Conclusion

This is the first report on the inflammatory response mediated cytotoxicity of HL 60 cells by ruthenium nanoparticles. Regulation of the balance between cell death inducers and inhibitors controls the apoptosis. High glycolic PLGA stabilized ruthenium nanoparticles are toxic to the human promyelocytic leukemia cells. These expressions of IL-1, IL-6, TNF-α, IFN-γ, FasL and the transcription factor NFκB that are significantly less compared to those of TGF β1, β2 and β3. With the human peripheral blood cells, there was a significant increase in the expression of NFκB, IFN-γ, FasL and TGF β1 and β3. Apoptosis in the case of HL 60 cells could be attributed to the increased expression of TGF β1, β2 and β3. We conclude that the signal transduction for apoptosis is also, but not only, through TGF β expression, which needs further investigation.

Acknowledgements

The authors acknowledge Dr Suresh Kumar Rayala, Associate Professor, IIT Madras for his help in intracellular ROS analysis and Mr Anbarasu, Molecular Virology Lab, IIT Madras for his technical inputs.

References

1 C. Y. Jin, B. S. Zhu, X. F. Wang and Q. H. Lu, *Chem. Res. Toxicol.*, 2008, **21**, 1871–1877.
2 T. Tsukatani and H. Fujihara, *Langmuir*, 2005, **21**, 12093–12095.
3 S. A. Love, M. A. Maurer-Jones, J. W. Thompson, Y. S. Lin and C. L. Haynes, *Annu. Rev. Anal. Chem.*, 2012, **5**, 181–205.
4 S. Veeraapandian, S. N. Sawant and M. Doble, *J. Biomed. Nanotechnol.*, 2012, **8**, 140–148.
5 S. N. Sawant, V. Selvaraj, V. Prabhawathi and M. Doble, *PLoS One*, 2013, **8**, e63311.
6 P. K. Prabhakar, S. Raj, P. R. Anuradha, S. N. Sawant and M. Doble, *Colloids Surf., B*, 2011, **86**, 146–153.
7 R. A. Wassel, B. Grady, R. D. Kopke and K. J. Dormer, *Colloids Surf., A*, 2007, **292**, 125–130.
8 A. N. Ananth, S. C. G. Daniel, T. A. Sironmani and S. Umapathi, *Colloids Surf., B*, 2011, **85**, 138–144.
9 J. Virkutyte and R. S. Varma, *Chem. Sci.*, 2011, **2**, 837–846.
10 C. Lu, C. Rice, R. Masel, P. Babu, P. Waszczuk, H. Kim, E. Oldfield and A. Wieckowski, *J. Phys. Chem. B*, 2002, **106**, 9581–9589.
11 S. U. Nandanwar, M. Chakraborty and Z. Murthy, *Ind. Eng. Chem. Res.*, 2011, **50**, 11445–11451.
12 X. Ni, B. Zhang, C. Li, M. Pang, D. Su, C. T. Williams and C. Liang, *Catal. Commun.*, 2012, **24**, 65–69.
13 O. Novakova, J. Kasparkova, O. Vrana, P. M. van Vliet, J. Reedijk and V. Brabec, *Biochemistry*, 1995, **34**, 12369–12378.
14 J. K. Barton, *Science*, 1986, **233**, 727–734.
15 M. Eriksson, M. Leijon, C. Hiort, B. Norden and A. Graeslund, *Biochemistry*, 1994, **33**, 5031–5040.

16 N. Grover, N. Gupta and H. H. Thorp, *J. Am. Chem. Soc.*, 1992, **114**, 3390–3393.
17 P. Mura, M. Camalli, A. Bindoli, F. Sorrentino, A. Casini, C. Gabbiani, M. Corsini, P. Zanello, M. P. Rigobello and L. Messori, *J. Med. Chem.*, 2007, **50**, 5871–5874.
18 T. Chen, Y. Liu, W. J. Zheng, J. Liu and Y. S. Wong, *Inorg. Chem.*, 2010, **49**, 6366–6368.
19 A. Castonguay, C. Doucet, M. Juhas and D. Maysinger, *J. Med. Chem.*, 2012, **55**, 8799–8806.
20 H. Qiu, J. Rieger, B. Gilbert, R. Jérôme and C. Jérôme, *Chem. Mater.*, 2004, **16**, 850–856.
21 V. Nandakumar, V. Geetha, S. Chittaranjan and M. Doble, *Biomed. Pharmacother.*, 2013, **67**, 431–436.
22 A. Thakor, J. Jokerst, C. Zavaleta, T. Massoud and S. Gambhir, *Nano Lett.*, 2011, **11**, 4029–4036.
23 S.-Y. Ho, W. Wu Jr, H.-W. Chiu, Y.-A. Chen, Y.-S. Ho, H.-R. Guo and Y.-J. Wang, *Chem.-Biol. Interact.*, 2011, **193**, 162–171.
24 F. Malik, A. Kumar, S. Bhushan, S. Khan, A. Bhatia, K. A. Suri, G. N. Qazi and J. Singh, *Apoptosis*, 2007, **12**, 2115–2133.
25 H. Pelicano, D. Carney and P. Huang, *Drug Resist. Updates*, 2004, **7**, 97–110.
26 B. Trouiller, R. Reliene, A. Westbrook, P. Solaimani and R. H. Schiestl, *Cancer Res.*, 2009, **69**, 8784–8789.
27 A. Sanchez-Capelo, *Cytokine Growth Factor Rev.*, 2005, **16**, 15–34.
28 T. Motyl, K. Grzelkowska, W. Zimowska, J. Skierski, P. Wareski, T. Paoszaj and L. Trzeciak, *Eur. J. Cell Biol.*, 1998, **75**, 367–374.
29 S. Edlund, S. Bu, N. Schuster, P. Aspenstram, R. Heuchel, N.-E. Heldin, P. ten Dijke, C.-H. Heldin and M. n. Landstram, *Mol. Biol. Cell*, 2003, **14**, 529–544.
30 N. Danker, K. Schmitt, N. Schuster and K. Krieglstein, *Gastroenterology*, 2002, **122**, 1364–1375.
31 M. Fogli, C. Carlo-Stella, A. Curti, M. Ratta, P. Tazzari, E. Ragazzi, S. Colla, A. M. Santucci, S. Tura and R. M. Lemoli, *Exp. Hematol.*, 2000, **28**, 775–783.
32 V. R. Baichwal and P. A. Baeuerle, *Curr. Biol.*, 1997, **7**, R94–R96.
33 C. Fan, J. Yang and J. F. Engelhardt, *J. Cell Sci.*, 2002, **115**, 4843–4853.
34 P. Bernabei, E. M. Coccia, L. Rigamonti, M. Bosticardo, G. Forni, S. Pestka, C. D. Krause, A. Battistini and F. Novelli, *J. Leukocyte Biol.*, 2001, **70**, 950–960.
35 D. De Stefano, R. Carnuccio and M. C. Maiuri, *J. Drug Delivery*, 2012, **2012**, 1–14.
36 M. Manikandan, N. Hasan and H.-F. Wu, *Biomaterials*, 2013, **34**, 5833–5842.
37 E. Porcel, S. Liehn, H. Remita, N. Usami, K. Kobayashi, Y. Furusawa, C. Le Sech and S. Lacombe, *Nanotechnology*, 2010, **21**, 085103.
38 A. O. Schueler, D. Flühs, G. Anastassiou, C. Jurklies, W. Sauerwein and N. Bornfeld, *Ophthalmic Res.*, 2005, **38**, 8–12.
39 V. Nandakumar, G. Suresh, S. Chittaranjan and M. Doble, *Ind. Eng. Chem. Res.*, 2013, **52**, 751–760.
40 C. W. Chen, C. Y. Chen and Y. H. Huang, *Int. J. Hydrogen Energy*, 2009, **34**, 2164–2173.
41 H. A. Jeng and J. Swanson, *J. Environ. Sci. Health, Part A: Toxic/Hazard. Subst. Environ. Eng.*, 2006, **41**, 2699–2711.
42 H. Chen, B. Zhang, Y. Yao, N. Chen, X. Chen, H. Tian, Z. Wang and Q. Zheng, *Molecules*, 2012, **17**, 13424–13438.
43 C. Jaya, V. Venkatesan and C. V. Anuradha, *Int. J. Biol. Med. Res.*, 2010, **1**, 120–124.